

**Ultrafast ultrasonic imaging of elastic properties in soft solids:
Application of speckle-interferometry to quasistatic
deformation**

Bachelor's thesis

submitted by
Julian Kühnert

at the University of Konstanz



Department of Physics

developed at the Isterre (Institut des Sciences de la Terre)
in Grenoble, France



1st supervisor: Prof. Dr. Georg Maret
2nd supervisor: Dr. Philippe Roux

Konstanz 2014

Abstract

The work investigates the deformation in soft solids by using pulse-elastography. Basis properties of soft solids are outlined as well as techniques, with which one can determine those properties. Different techniques are presented to process data of a ultrafast ultrasonic imaging device, including a cross-correlation method, an amplitude-extracting method and a phase-extracting method. The two latter are tested with the help of a computer-simulated signal. Finally, several deformation experiments on a gel-based soft solid in different conditions and of different parameters are presented. The results are discussed and a general conclusion is made, evaluating the different processing techniques and suggesting further investigations.

Zusammenfassung

Die vorliegende Arbeit untersucht Deformationen in weichen Feststoffen mittels einer Puls-Elastographie Technik. Die Hauptmerkmale von weichen Feststoffen werden ebenso besprochen wie verschiedene Techniken, die in der Lage sind, die Eigenschaften von weichen Feststoffen festzustellen. Anschließend werden verschiedene Methoden zur Datenauswertung vorgestellt: eine Kreuzkorrelations Methode, eine Methode, die die Amplitude der aufgenommenen Signale nutzt und eine, die die Phase der Signale nutzt. Die zwei letzteren werden mit Hilfe computergenerierter Daten getestet. Schließlich werden verschiedene Deformations Experimente an einem gel-artigen Feststoff unter verschiedenen Konditionen und mit verschiedenen Parametern ausgeführt. Die Ergebnisse werden präsentiert und besprochen. Eine allgemeine Schlussfolgerung bewertet die unterschiedlichen Methoden zur Datenauswertung und präsentiert Vorschläge zur weiteren Behandlung der Thematik.

Contents

1	Introduction	3
2	Elastic moduli and elastography	4
3	Experimental Gel Bulk: Properties and Production	7
4	Ultrafast ultrasonic imaging and speckle interferometry	8
5	The processing techniques	11
5.1	Cross-correlation method	11
5.2	Amplitude-extracting method	12
5.3	Phase-extracting method	14
5.4	Correction for non-directional backscattering	14
5.4.1	Smoothing of channels	14
5.4.2	Beam forming	15
6	Preparations: Experimental set-up and test simulations	16
6.1	Experimental set-up	16
6.2	Inspection of novel methods by simulation	17
7	Experimental results	19
7.1	Linear deformations	20
7.2	Linear deformations with fixed point	22
7.3	Linear deformations with friction interface	26
7.4	Oscillatory deformations	29
8	Conclusion	32
References		34
List of figures		35

1 Introduction

Ultrasonography is widely used for medical applications. Pulses of ultrasound, which is characterised by frequencies above the human hearing range, are sent into body tissue. The pulses are reflected for example by organs, bones and blood streams in different ways, which makes it possible to visualise the internal body and to obtain physical properties of its tissues by analysing the recorded echoes in amplitude, frequency and travel time.

By correlating the echoes of successively sent pulses one can also follow the development of the location of reflectors, and thus, the development of deformation or shear inside soft solids, characterising their elasticity. This method is called pulse-elastography or transient elastography. Sandrin *et al.* [2] used this technique to visualise the propagation of a shear wave in a plane inside a tissue-mimicking gel-based phantom using ultrafast ultrasound, i.e. successive ultrasound pulses at very high rate. Shear waves (S-waves) are transverse waves inside elastic media, which means that they oscillate, in contrast to pressure waves (P-waves), perpendicular to their travel direction.

As S-waves appear also as body seismic waves after earthquakes, the pulse-elastography technique is highly attractive to study rupture dynamics in soft solids in order to simulate and understand processes in seismology. Latour *et al.* [3] used the technique to study dynamic sliding friction by observation of S-wave propagation in soft solids after slipping events on frictional interfaces. More explicitly, they located a gel-based phantom on undergrounds with rough surfaces and observed the dynamics in the gel right above the interface, while the gel is pulled along the plate. Consequently, areas of the gel temporarily stuck to the rough surface and will slip, when the stress field is stronger than the friction force. As a result they found two different types of slipping regimes which had also been observed in seismic events. In a more recent study [4], they expanded their observations, adding heterogeneities in the frictional interface. By this, barriers are created, which interact with the rupture propagation. Besides different interactions of various types of barriers, which agree with previous numerical simulations, they also concluded, that the complex and unpredictable processes of seismic ruptures have at least partly to be explained by heterogeneous prestress from earlier events.

However, before understanding the heterogeneous stress field which will cause rupture events, one has to go at least one step back and make observations on the deformation in the medium which then causes a stress field.

The aim of this work is to visualise the deformation field in a medium, which is deformed by external pressure. As a medium, a gel-based soft solid is used, allowing it to detect internal displacements by pulse-elastography. Several deformation experiments are carried out at scale of laboratory and are evaluated in order to provide tools to study the behaviour of soft solids. By this, this work wants to contribute to current research by showing a way to visualise deformation inside a medium, in order to simulate complex problems experimentally, such as the above mentioned heterogeneous prestress, which causes the unpredictability of rupture events.

As a basis, elastic properties of soft solids and the state of the art techniques,

which are present in the medical field to examine internal body structures, are outlined in the following. Afterwards, the properties of the gel-based soft solid which is here used in the experiments is presented and how it is prepared. How the interior of this medium is inspected by pulse elastography is introduced afterwards, followed by the presentation of different signal processing techniques: the method of cross-correlating time-windows of successively recorded echoes and two novel methods, extracting either the amplitude, or the phase of the signals and following their development over the successively recorded frames. At this point, the whole theoretical basis is discussed and the experimental studies are prepared. The set-up of the experiments is explained and first simulations are done, in order to test the novel processing techniques. Then, several deformation experiments are carried out under different conditions and parameters. The experimental results are discussed, including an evaluation of the different processing techniques. Finally, a general conclusion on the results is made and further research with the same experimental configuration is suggested.

2 Elastic moduli and elastography

Ever since, medical practitioners have examined internal body structures by palpation, trying to discover unhealthy tissue and evaluate it qualitatively. This evaluation is not only dependent on the experience of the physician, but also has its limits in the position, the size and the type of the examined object. Thus, a stronger examination method is on demand, with which one can image internal structures and quantify their properties, but still without intervention into the body. Ultrasonography is an important tool to get an insight into the body by evaluating the echoes of ultrasonic pressure waves. The reflection of those waves is principally dependent on the compressibility κ of the tissue, which influences the pressure wave velocity c_P by the relation $c_P^2 = 1/\rho\kappa$, with the density ρ of the material, and thus, also influences the acoustic impedance $Z = \rho c_P$. The compressibility of a homogeneous isotropic soft solid (which will be assumed from here on) can be determined by the bulk elastic modulus B by $\kappa = 1/B$. This also simply called bulk modulus of a soft solid expresses its frictional volume change $\Delta V/V$, when exposed to a uniform compression $p = F/A$ from all directions of force F on its whole surface A :

$$B = \frac{F/A}{\Delta V/V} = \frac{\text{uniform compressure}}{\text{frictional volume change}} \quad (1)$$

The bulk modulus is an extension to three dimensions of Young's modulus, which quantifies the stiffness of an elastic material by its deformation along one axis $\Delta l/l$, due to opposing forces F along the same axis on a perpendicular area A (see figure 1, left):

$$Y = \frac{F/A}{\Delta l/l} = \frac{\text{normal stress}}{\text{normal strain}} \quad (2)$$

But there is another elastic modulus to characterize soft solids by quantifying their resistance to deformation through a stress-to-strain relation. The shear

modulus G investigates the elasticity of a soft solid, in other words how much an elastic bulk of length l is deformed or sheared, when opposing forces F work tangential to opposite surfaces A (see figure 1, right):

$$G = \frac{F/A}{\Delta l/l} = \frac{F/A}{\tan \gamma} = \frac{\text{shear stress}}{\text{shear strain}} \quad (3)$$

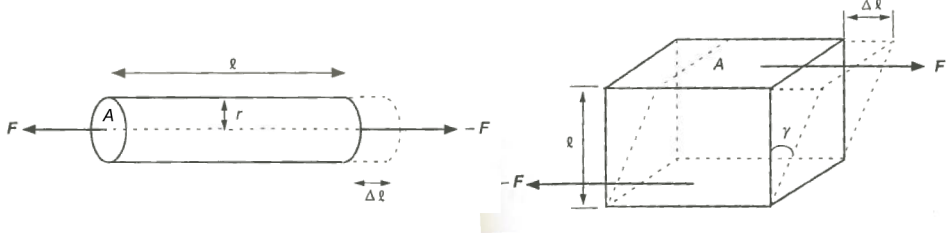


Figure 1: Illustration of the definition of Young's modulus (left) and shear modulus (right) (extracted from [7]).

As the shear modulus provides information about the elasticity of soft solids, it opens a door to inspect tissue's hardness and thus, to gain contrast in the structural image of the internal body built up by ultrasonography. The investigation of the elasticity of soft solids is generally termed as elastography. Its foundation was formed in the 1980s by the method of sonoelastography, in which tissue is stimulated by low frequency vibrations. Their propagations through the tissue is then imaged using an ultrasound technique. Further developments were rapidly made, creating among others the here used pulse-elastography technique and also the magnetic resonance imaging technique (MRT), where magnetic fields and radiowaves are used instead of ultrasound. Sarvazyan *et al.* [1] summarized, that elastography 'provides the physician with a virtual finger', pointing out the use of elastography as a quantified palpation method. Furthermore, they stressed the potential of elastography by revealing the large variation of the shear modulus in contrast to the bulk modulus in soft solids. In figure 2 you can see the variation of the bulk modulus and the shear modulus of several tissues depending on the exposed pressure. It is clearly visible, that the examination of the shear modulus makes a differentiation of the tissues over a wider range possible, than examining the bulk modulus. This can be of high importance to reveal for example areas of unhealthy tissue.

As an example how useful elastography is for medical purposes, figure 3 shows an examination of a liver, that contains a tumour. The right side shows the image of an usual ultrasonography. By real-time tissue elastography (presented in [7]), a method where the tissue is compressed and released in several cycles by external forces, one can gain contrast in the image. As the tumour is harder than the surrounding liver tissue, it doesn't undergo so much strain while compression. This property can be visualised by the elastography method and is mapped in colours above the ultrasonography picture, whereas blue corresponds to hard tissue and red to soft tissue.

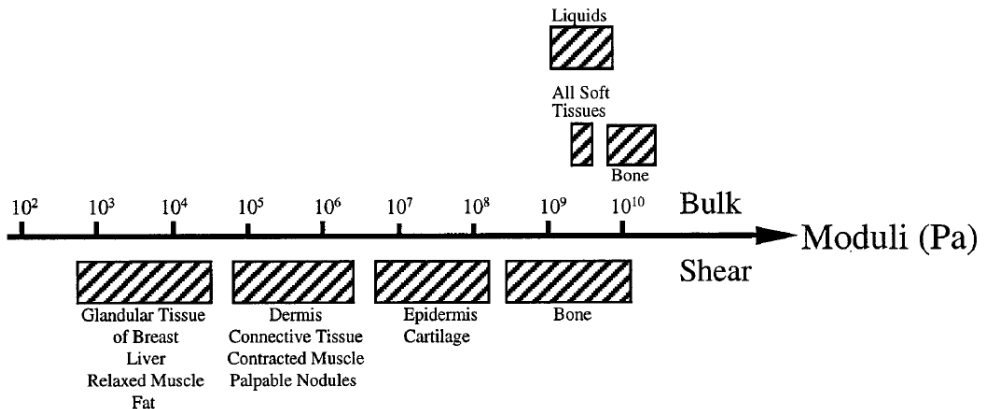


Figure 2: Bulk- and shear moduli of different tissues, dependent on the applied pressure (extracted from [1]).

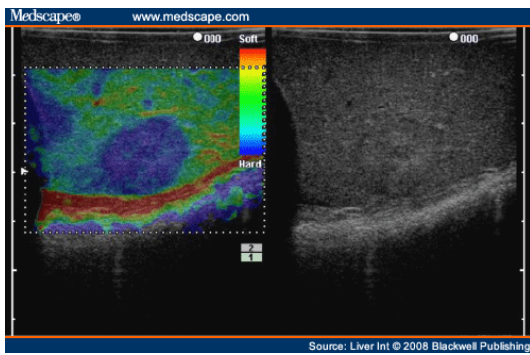


Figure 3: Real-time tissue elastography (left) is used to detect a tumour inside the liver, which cannot be resolved by ultrasonography (right). The tumour is visible in blue colour, as it is harder than the surrounding liver tissue (extracted from [7]).

Pulse-elastography studies the elasticity of soft solids by following internal movements. Ultrasonic pulses are sent into the medium successively, and each echo is compared to the one of the next pulse. If there is no movement at all in the medium, the echoes are the same. If there is a movement, you can see differences in the echoes. The rate of the sent pulses is limited to the time at which the last reflected signal is recorded. A higher rate would cause interferences of the echoes, thus distorted signals.

Given a soft solid of low compressibility, i.e. high bulk modulus, the pressure wave speed is high (as discussed above: $c_P^2 = 1/\rho\kappa = B/\rho$), what consequently enables to work on a high pulse rate, in other words to get information from inside the medium very quickly. If, additionally, the soft solid is highly elastic, quantitatively characterised by a small shear modulus G , the shear wave velocity is small (analogue to the pressure wave velocity: $c_S^2 = G/\rho$). Having $c_P \gg c_S$ ($c_P/c_S \sim 10^3$, [5]), one can follow the shear wave propagation using ultrasonic imaging. This opportunity has been used in several studies to investigate physical properties, e.g. rupture dynamics as already mentioned in

the introduction [3],[4].

In this work, the same approach is used to study elastic properties of soft solids, whereas the focus is laid on quasistatic deformation, which means that the deformation is not influenced by any dynamic effect. Besides, the deformation field is described solely qualitatively, as the investigations are concentrated on different processing techniques and the illustration of deformation experiments of different parameters under different conditions.

3 Experimental Gel Bulk: Properties and Production

The deformation experiments are carried out on gel-based, linear elastic soft solid bulks. Those homogeneous bulks consist mainly of water, which is held by tangled polymeric polyvinyl alcohol (PVA) chains. The high percentage of water (up to 95 %) gives them a low compressibility, making pressure wave velocity in the medium very high ($c_P \approx 1500 \text{ m/s}$ as in water). This allows the use of ultrasound imaging at a high rate. Furthermore, previous experiments on this kind of hydrogels show, that their highly elastic character, caused by the PVA chains, can be used to study physical behaviours such as dynamic friction and shear wave propagation with results comparable to observations made on earthquake events [3],[4].

Deformation of the hydrogel is observed by backscattered signals of the ultrasonic pulse from scattering particles inside the medium. A low volume percentage of cellulose particles serve as scatterers. Having a scattering cross-section which is smaller than the wavelength of the ultrasonic pulse, they scatter only part of the energy, allowing to treat the recording signals in a single scattering regime (further explanations in section 4).

The production of the gel has to be carried out carefully in a strict order to avoid undesired effects. At first it is recommended to mix PVA powder with the cellulose particles to ensure a uniform distribution of the scatterers in the gel. For 1 L of water, 100 g of PVA powder is needed. The amount of scattering particles can be varied on demand: higher amounts of scatterers create stiffer gels (stiffness depends on material density) and a denser backscattered signal. For small amounts the gel behaves vice versa. For the experiments here, gels with amounts of cellulose particles between 1 g and 18 g were created.

The mixed powder is afterwards slowly added to 1 L of water while stirring to avoid lumps of PVA grains which can easily stick together at higher temperatures. As soon as it is well mixed, it is heated up while stirring to a temperature of almost 90° C (below boiling point), which it has to keep another 3 hours in which the PVA slowly melts and builds a viscous liquid with the water. Here it is important to continue stirring, as the powder would otherwise settle down to the bottom and would not build a mélange with the water.

After this is done, the liquid is ready to be filled in a mould of desired shape and to be cooled down to room temperature. This is followed by a cycle of freezing to -20° C for at least 24 hours and thawing, in which a crystallization of the gel takes place. To avoid cracks in the gel while unfreezing due to stress

release from expansion of the liquid inside the acrylic glass mould, it is best to put the gel within the mould into ice water and let it defrost very slowly. The defrosted gel bulk is ready for use. By adding cycles of freezing/thawing, it is possible to increase the crystallinity and thus the stiffness of the gel. As water vaporizes out of the hydrogel when being in air, the bulk has to be stored in water to not dry out within a couple of hours.

4 Ultrafast ultrasonic imaging and speckle interferometry

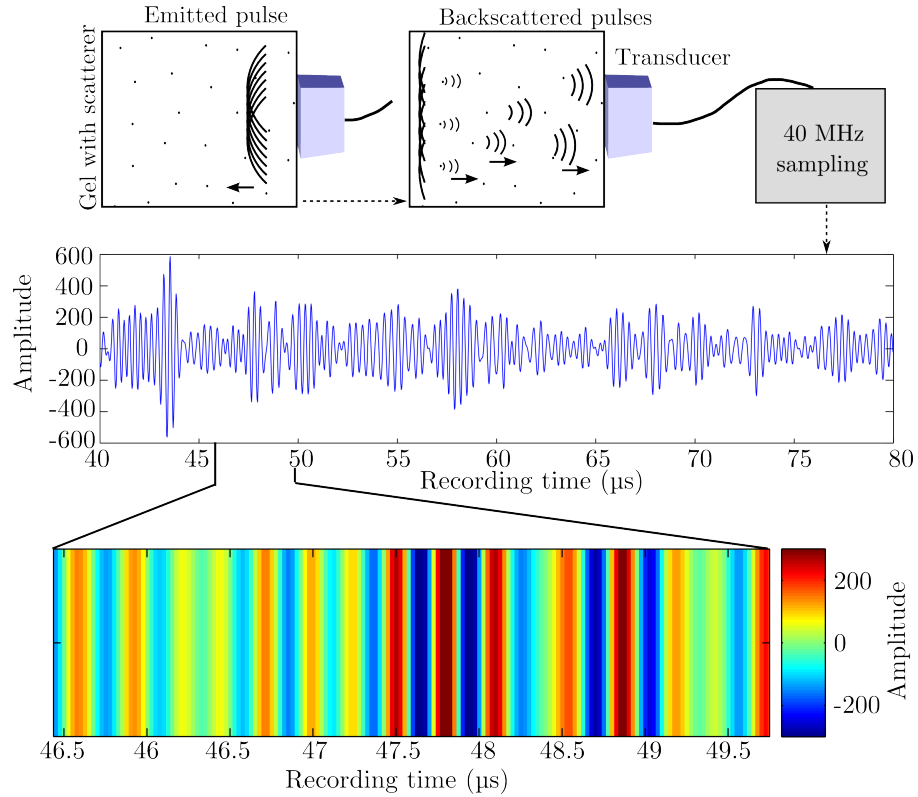


Figure 4: Illustration of the imaging technique: a transducer array is emitting a pulse into the scattering medium. Backscattered signals arrive at different times by the same array. The signals are sampled at 40 MHz. The image in the middle shows the so recorded signal in one channel. The bottom image contains the same informations of a zoomed time section. This record will form with the records of the other channels the so called speckle pattern.

To carry out pulse-elastography, a device is needed to send pulses and record the echoes. Here, a multichannel device with an array of 64 transducers is used. The transducers are ultrasonic sensors with the ability to emit and receive ultrasonic signals.

To now examine physical properties, the array is held directly onto the surface of the soft solid (here the gel bulk which was described in section 3). Using

a contact gel in the interface, reflection of the pulse on air, which might be enclosed in between the surfaces, is avoided. An ultrasonic pulse, sent out from a transducer, will then penetrate into the medium as a circular pressure wave (regarding the plane of interest in front of the array). By sending off pulses at all the transducers simultaneously, a pressure wave with a planar wave front will form in front of the array (see figure 4). The pulse travels through the medium at pressure wave speed c_P and is partly scattered by the randomly located cellulose particles. The backscattered signal of a scatterer, located at distance d from the array is recorded by the highly directional transducers at time $t = 2d/c_P$ after the pulse was sent into the medium. The signal, recorded by the corresponding transducer, within a short time window around this time t , is determined in amplitude and phase by constructive and destructive interferences of backscattered signals from the particle and its closest neighbours. This way, an interference pattern, also called speckle pattern, is created by the recordings of the 64 transducers. The total recording time after each pulse shot defines the investigated depth inside the medium. Figure 5 illustrates the speckle patterns after several recordings. The patterns correspond to a plane inside the medium of width similar to the transducer array and depth defined by the recording time.

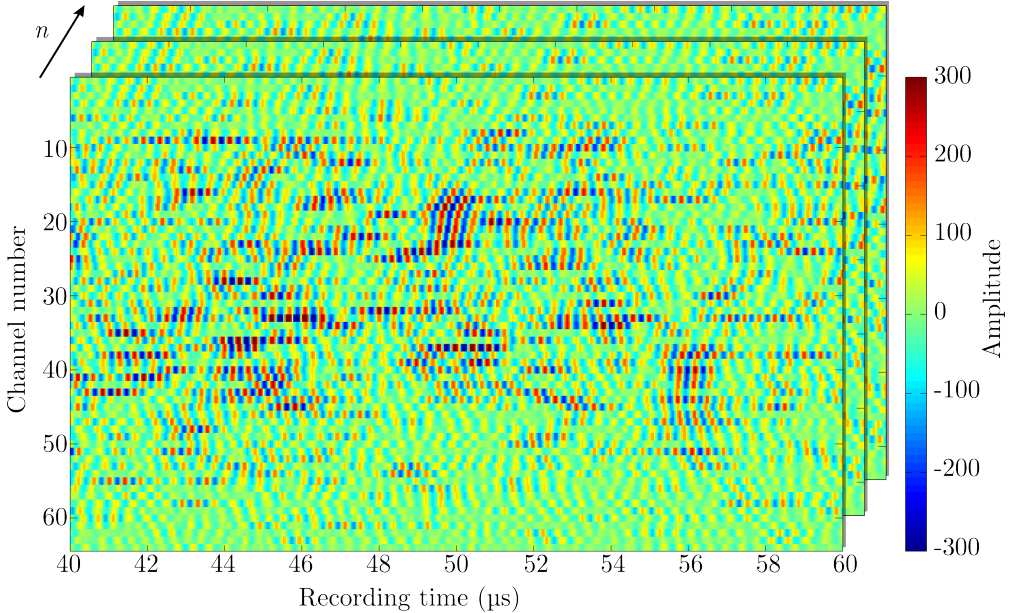


Figure 5: Illustration of the speckle pattern created by backscattered pulses, received by 64 channels over a defined recording time. This pattern is created after each of n successive sent signals.

As the speckle pattern is determined by the distribution of the scatterers inside the medium, it stays exactly the same after successively sent pulse shots, as long as the scatterers stay in the same position. However, if there is a movement inside the medium, changing the distance of the scatterers to the array, the pattern will change as well, as the signals are recorded earlier or later. This can be seen in figure 6, which shows the recorded signal in a

linear of one channel over $n = 40$ recording shots, where a linear displacement is started after the fifth shot.

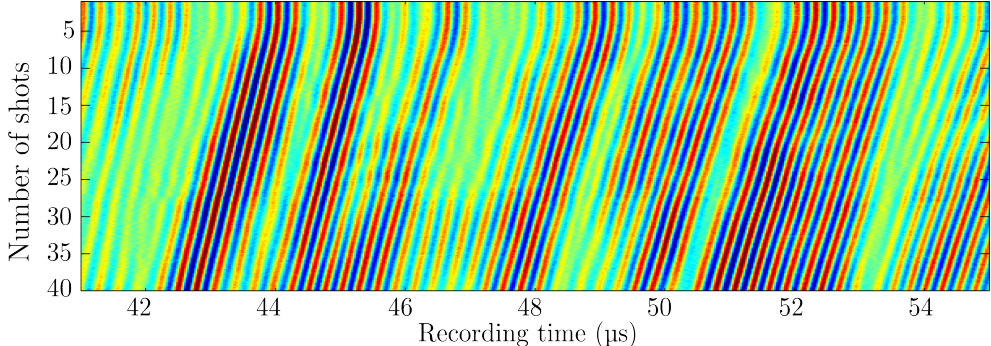


Figure 6: Change of a speckle signal over 40 frames, received by one channel.

The time delay of a characteristic signal from a group of scatterers between two successive recordings can be retrieved and directly gives information on movements of this group, as the travel speed of the signals is well known. By this, the displacement field, and thus the deformation field inside a soft solid along the axis of the pulse emission direction can be reconstructed.

The signals are processed in a single scattering regime, which means that it is assumed, that recorded signals are only scattered once, forming a forth and back travel path. This assumption is valid inside media, in which the scattering mean free path, that describes the mean travel distance of the pulse, which it can pass without being influenced by a scatterer, is longer than the length of the recording depth. As it is difficult to determine the exact mean free path of a medium, which is dependent on the density of the scatterers and their scattering cross section, we can validate the assumption experimentally by recording the reflection of an interface behind the studied soft solid. If the amplitude of this reflection is of way higher magnitude than the general scattering amplitude inside the gel, we can conclude that only small parts of the initial pulse energy is scattered inside the gel, what led us assume a single scattering regime. Figure 7 show the result of this experimental test, which was carried out on the gel with highest amounts of scatterers (cellulose particles) and a metallic plate behind the gel at about 80 mm distance from the transducer array. The reflection of the metallic plate is clearly visible in the speckle pattern (beginning at about 102 μs) and much stronger than the backscattered signals from the particles in the gel. This result clearly allows the single scattering regime.

The single scattering assumption can also limit the recording depth. However, for the soft solids in the here described experiments, the recording depth is rather limited by the scattering amplitude. Working with emitted pulses of 50 V, reflections are no longer strong enough seen at about 10 cm depth to form analysable interference patterns. As already mentioned earlier, further limitations concern the pulse rate. The previously sent pulse has to die out in the medium completely before the next pulse can be sent. Otherwise,

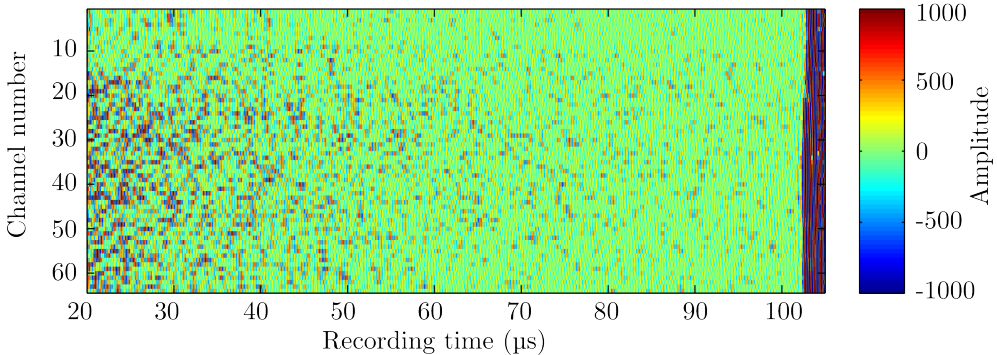


Figure 7: Proof of the single scattering regime in the gel by visualization of the strong reflection from a metallic plate behind (from $102\ \mu\text{s}$ on).

mixing of the reflections and therefore distortions of the recordings can arise. Nevertheless, as the pressure wave speed is very high in the here used gel-based soft solids, pulses travel quickly making pulse rates up to 2000 Hz possible. This is even enough to follow shear wave propagation. However, as quasistatic deformation is investigated in the experiments, it is sufficient to send pulses at a rate between 250 Hz and 350 Hz. Besides, the used transducer array is designed to work at a central frequency of 3.5 MHz, holds 64 transducer sensors which are distributed over a length of 48 mm, i.e. in 0.75 mm distance from each other. Furthermore, the reflections in between the pulse shots are recorded with a sampling frequency of 40 MHz.

5 The processing techniques

After recording the reflections after n emitted pulse shots, which each form a speckle pattern of width of the 64 channels and length of the recording time in units of sampling points, there are different ways to analyse the data: the commonly used cross-correlation method and two here developed methods using either the amplitude or the phase of the signals.

5.1 Cross-correlation method

The cross-correlation method compares the signals of two successive frames in a defined time window and finds mathematically the position where they are most congruent, by shifting them against each other and integrating their product after each shift. Figure 8 shows two successively recorded signals from a scattering medium, in which the scatterers were displaced in between the shots. The displacement can be recognized by the time delay between the two signals.

The shift, which leads to the most coherent position of the two signals in the correlation, corresponds directly to the time delay between them and thus the displacement inside the medium. Given the data X_t and Y_t of two successive shots at recording time t , the cross correlation within a time-window T around

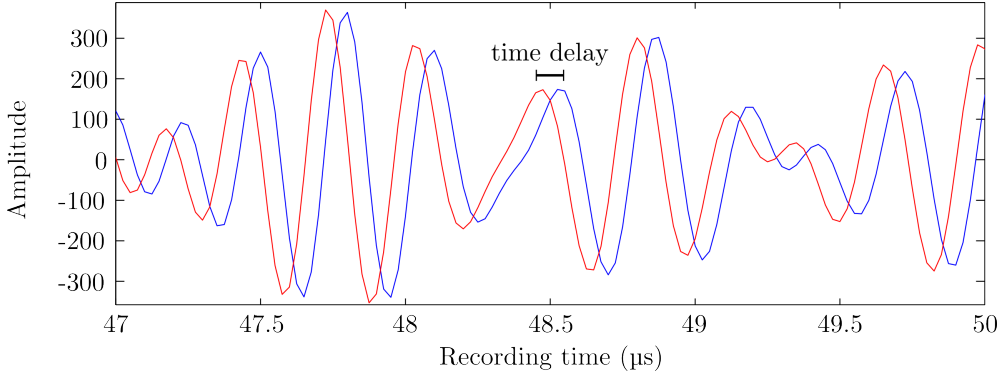


Figure 8: Backscattered signals of two successive pulse shots in a scattering medium, which is displaced in between the shots, causing a delay of the signals in the recording time.

t is explicitly written as follows:

$$(X_t \star Y_t)_{\tau} = \sum_{t=-T}^{T} X_{t+\tau} Y_t^* \quad (4)$$

The argument of the maximum of the cross-correlation function determines the time delay between the two signals: $\Delta\tau = \text{argmax}_{\tau} (X_t \star Y_t)_{\tau}$.

What is left to do is to calculate from the delay in units of sampling points the real displacement in units of distance:

$$\Delta d = c_P \cdot \frac{\Delta\tau}{2} \quad (5)$$

The time window has to be defined similar to the size of the used pulse length. Like this, backscattered pulses from the particles can be evaluated and the single movement of regions can be detected. To evaluate the whole recording time, the time window is slightly shifted along the entire array, while cross-correlation is carried out after each shift. Doing this, the speckle pattern is transformed into a displacement field, which shows the displacements inside the medium in a plane in front of the array. Calculating the cumulative sum of the displacements at each position of the plane over successive shots gives finally the deformation field.

5.2 Amplitude-extracting method

The amplitude-extracting method follows the development of one speckle point over the successive shots of a measurement at a chosen position in the interference pattern. Without any deformation in the Gel the amplitude of a speckle point stays at the same level within some noise fluctuations. A deformation causes a change in the backscattered signal and thus a change in the amplitude of one speckle point. For instance for a linear displacement, the amplitude of the speckle point oscillates (see figure 9, top).

These oscillations correspond to a vertical top to bottom walk in figure 6.

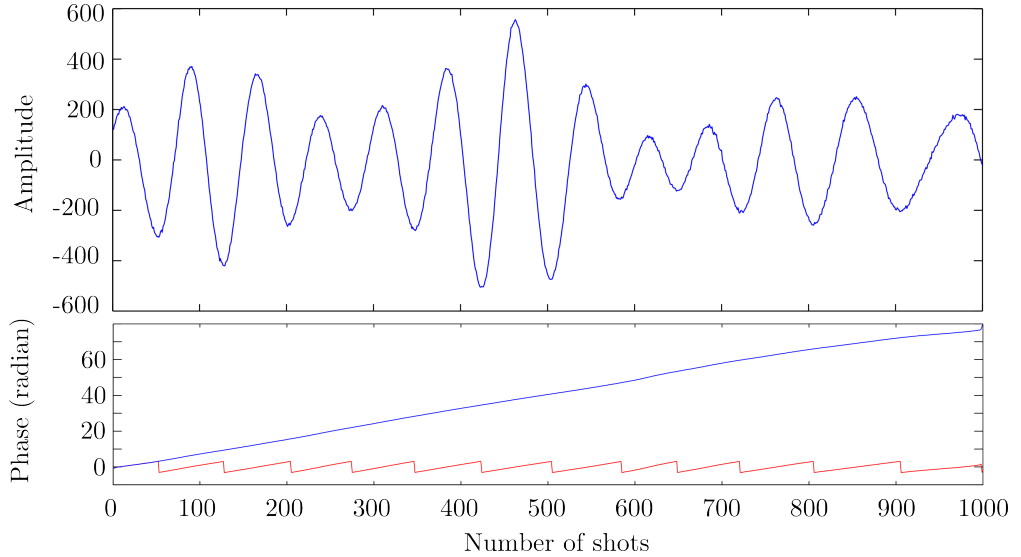


Figure 9: On top the oscillations of one speckle point during a linear deformation experiment of $n = 1000$ signal emitting-receiving cycles. Bottom image shows the corresponding wrapped phase (red) and absolute phase (blue).

Following a full oscillation means, that the position inside the medium corresponding to this speckle point is displaced about one wavelength in units of the originally sent pulse. By counting the number of oscillations one finds out the total displacement.

One way to count the number computationally is to extract the phase of the oscillations. The unwrapped (absolute) phase over several frames can then be translated into the displacement at the corresponding position inside the medium. With the help of a Hilbert transform, the recorded signal can be converted into a analytic signal, from which the phase can be extracted. If the spectrum of the signal is not too broadband, but concentrated on a low frequency band, the output of this Hilbert transform can be written as

$$A(t) = \hat{a}(t) \cdot e^{i(\omega t + \varphi(t))} =: \hat{a}(t) \cdot e^{i\phi(t)}, \quad (6)$$

which describes the time dependent signal $A(t)$ by a real amplitude $\hat{a}(t)$ and complex phase $\phi(t)$. The bottom image of figure 9 shows the in this way extracted phase of the oscillation on top, while the red curve corresponds to the phase wrapped in between $-\pi$ and π and the blue curve corresponds to the absolute phase.

However, especially for small displacements smaller than a full wavelength or oscillatory displacements, exact counting is difficult to realize.

When it comes to oscillatory movements of the gel, the method also faces problems, as the amplitude oscillations described above are not necessarily here visible (imaging a oscillation around the flat peak of the pulse in contrast to the oscillation around the steepest part of the pulse). What seems here to be more appropriate is matching the speckle amplitude to the one of the original pulse. In order to do this, it is important to normalize the interference pattern. By finding the corresponding amplitude of the backscattered signals

to the original pulse, an exact pulse position information can be assigned to each sampling point. The normalization is done by dividing the signal by its envelope. The envelope is determined by the absolute of the Hilbert transformed signal $A(t)$. Now each point of the signal can be compared with the normalized pulse, whereas only one slope from -1 to 1 of the pulse is taken to avoid multiple matching. This in turn demands for some further processing to derive the slope in between the sampling points. In order to do so, the Fourier transform of the just created array is calculate, in which the whole spectrum of frequencies is shown. Limiting the spectrum up to the lowest frequency peak, and going back to time-space by the inverse Fourier transform reconstructs finally the oscillation of the gel at the position corresponding to the speckle point. The amplitude of the oscillation has to be determined by transferring the energy of the whole frequency spectrum into the limited frequency spectrum. It is to mention, that this processing method as it is described here is only applicable to linear oscillations. Furthermore, the initial direction of the oscillation is left to be determined.

5.3 Phase-extracting method

In contrary to the amplitude-extracting method, we now make use of the instantaneous phase of the recorded signals. With the help of the already above used Hilbert transform, the phase is directly obtained. For a linear displacement, one can now follow the absolute phase in one speckle point over successive frames. Phase shifts tells about displacements of scatterers. As the wavelength of the pulse is well known, the phase shift can easily be translated into displacement in distance.

However, the limitations of the amplitude-extracting method are here true as well. That is why for an oscillatory movement of the medium the same procedure as above is applied, first limiting the frequency spectrum of the signal and then transferring the whole energy into this frequency band.

5.4 Correction for non-directional backscattering

As the particles scatter the pulse in all directions, the backscattered signal is not necessarily recorded by only one receiver channel, even though the transducers are highly directional. Thus, there is need to correct the signal processing in a way, that the channels are not treated separately any more. In the following, two correction methods are presented.

5.4.1 Smoothing of channels

A simple way to connect the receiver channels to process an image of the deformation of the medium which is probably closer to reality, is to overlay the data of neighbouring channels. This is done by simply adding the signals of a number of channels to the current channel, which will afterwards be treated as usual. Figure 10 illustrates the problem, that the backscattered signal of one scatterer is recorded by multiple channels and shows the described smoothing method.

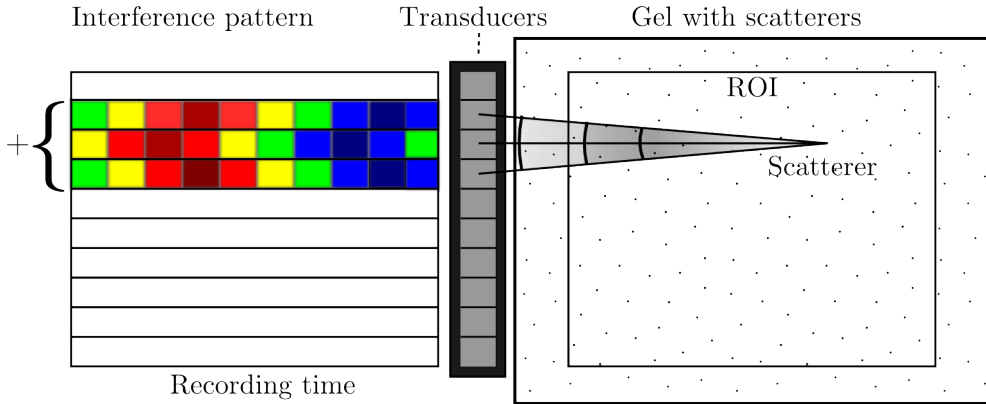


Figure 10: Smoothing of channels by overlaying them, as they receive the backscattered signal of the same scatterer.

5.4.2 Beam forming

Another, more complex way to connect the signals of the channels will especially be important, when single strong scatterers or scattering areas are present in the medium. The beam forming technique tries to project back the recorded signals to their origin and thus reconstruct the scattering medium. This is done in a way, that the resulting speckle pattern, which now represents directly the location of the scatterers, still contain the phase and amplitude information of the backscattered pulse.

First step is to choose a focal area in which the signals of the channels are backprojected. Given a length D of the transducers array and a focal length F between the array and the scatterers, the dimension of the focal area is not longer than $\sigma_l \sim 8\lambda(F/D)^2$ and not wider than $\sigma_w \sim \lambda \cdot F/D$.

After that, one has to calculate the time delay δt , with which the backscattered signal arrives in the different channels. The directional backscattered signal travels the shortest way and thus arrives first at the corresponding channel. The other channels receive non-directional backscattered signals after a delay according to the longer travel distance. This is illustrated in figure 11.

To focus the signal (the beam) back to its origin, we shift the channel recordings about the before calculated delay. As it is of big computational effort to shift all the data points of the signal arrays, we go by Fourier transform to frequency space, where we can simply multiply by the time delay. The following formula holds to calculate the by δt shifted signal X_{Ch} of one channel, where $F(\omega)$ is the Fourier transformed and ω the frequency of the signal:

$$X_{Ch}(t + \delta t) = \frac{1}{2\pi} \int_{-\infty}^{\infty} F_{Ch}(\omega) e^{2\pi i(\omega \cdot \delta t)t} dt \quad (7)$$

After shifting the signals according to the delay, we go back to time space where we can simply choose the signal interval, which corresponds to the current focal area (see figure 12). Before overlaying the channels, their signal amplitude is weighed in order to put more emphasis on the channel which receives the directional backscattered signal and to weaken the channels which

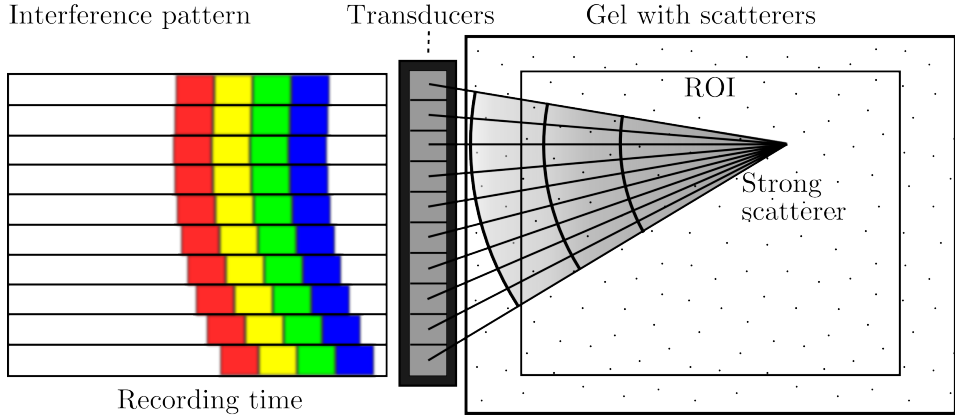


Figure 11: Backscattered signal of a strong scatterer is received in many channels and thus causes the requirement of beam forming.

are further away from the scatterer and thus receive a more damped signal. This is mathematically done by a Hann function. This window function is very appropriate here, as it is sharp enough to focus well without losing too much resolution, but at the same time it is smooth enough to avoid the creation of side lobes. Also, it is possible to select the number of contributing channels by choosing the width of the window.

The entire process is done until the whole scattering area is reconstructed.

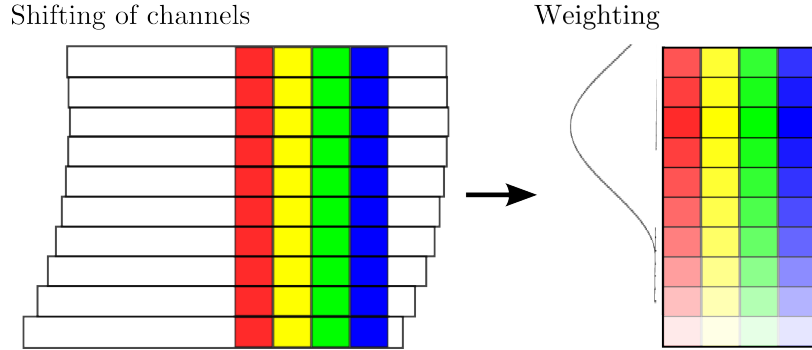


Figure 12: According to the delay in arriving of a signal between the channels, the data is shifted. Before overlaying them, the signal amplitude is weighed, putting more emphasis on the channel that receives the directional backscattered signal.

6 Preparations: Experimental set-up and test simulations

6.1 Experimental set-up

The deformation experiments are carried out in a simple set-up, which is illustrated schematically in figure 13. The most important characteristic is,

that the gel is located in between two edges: one locked edge, i.e. locked in respect to the transducer array and thus without change of position during the measurement, and one moving edge, which will compress or decompress the gel. The moving edge is driven by a motor which can be controlled from a computer (linear as well as oscillatory movements can be carried out). The transducer array is located at the locked edge, whereas one can change its position to either investigate a horizontal or a vertical plane in the medium. The interfaces between the gel and the plates on top and bottom (the bottom one is moving with the pushing edge) are provided with water, in order to make them frictionless (if friction is not specially wanted). Nevertheless, an amount of friction cannot be avoided and will be included in the evaluation of the results if needed. There is the possibility to put weight on the top plate to either stop the gel from expanding in this direction or to provide normal pressure to carry out an experiment with frictional interface. Furthermore, the position of the moving edge can be measured by a laser, what can be used later as a reference in the experimental results.

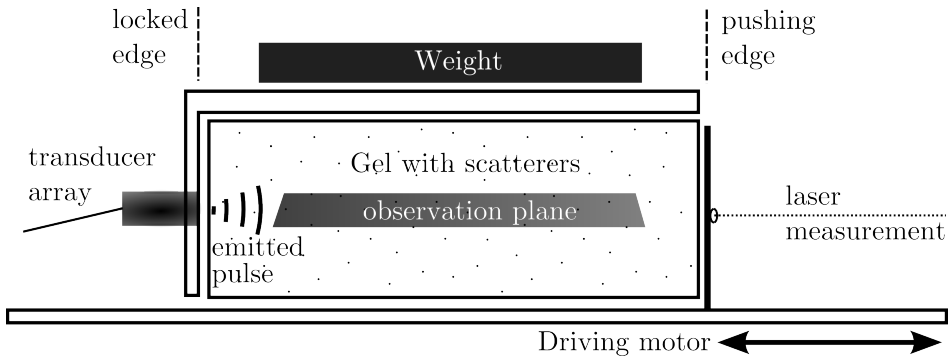


Figure 13: Sketch of the experimental set-up.

6.2 Inspection of novel methods by simulation

This section wants to reveal problems of the amplitude- and phase-extracting methods, by testing them with the help of simulated signals. To do this, speckle patterns are produced in size of one channel, and shifted according to a linear or an oscillatory deformation (data comparable to illustrations in figure 6 and 30, respectively). Furthermore, signal noise can be added to detect limitations for the treatment of experimental data.

First of all, we are look at the analysis of linear deformation data. Given a very small displacement, the amplitude-extracting method has difficulties to detect the true displacement. The change of the amplitude in the single speckle points during the recording is so small, that any kind of noise level leads to the case, that the method recognizes fake oscillations and interprets them as displacement of the scatterers. For larger linear displacements it is different. The changes in amplitude of the speckle points over several frames are much more determined, making it easy for the method to count oscillations and assigns them to the right displacement.

For the phase-extracting method it seems to be vice versa. It can only analyse

very small displacements in a good manner, for larger displacements the phase of the signals changes too much from one shot to the next, making it impossible for the method to follow. Figure 14 illustrates this problem by showing a usual result of the phase-extracting method for large linear displacements: phases of the signals are mismatched from one shot to the next, causing a fake jumping displacement instead of a linear displacement.

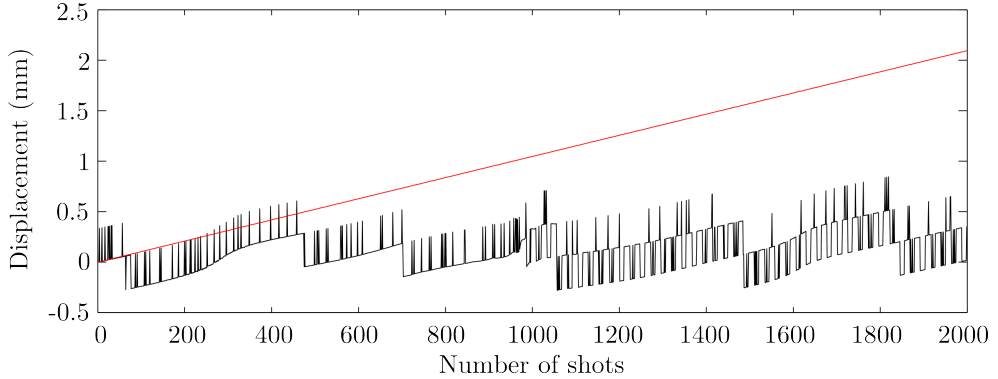


Figure 14: Testing the phase-extracting method in a simulated linear deformation experiment. Red: the actual simulated displacement, black: the result of the analysis by the phase-extracting method.

What is left to mention is that the direction of the displacement cannot be revealed by the methods. Instead, they always give the same direction. To solve this, one has to add another parameter, which determines the direction, e.g. by comparing the development of two neighbouring speckle points.

Now we have a look at the analysis of oscillatory displacements, where we apply the trick of choosing the oscillation frequency from the spectrum. Figure 15 shows steps of the analysis by the amplitude-extracting method. The red curve is the simulated oscillatory displacement. After normalising, the method matches the amplitudes of the signal to the pulse amplitude to get a position. The blue curve shows the resulting array. From this array, one has to extract the low frequency band and transfer the energy of the entire spectrum to this band to finally reconstruct the oscillation movement, which is shown by the black curve in the figure. The image illustrates the general result of the test simulation: the displacements could be relatively good reconstructed even for small displacements in which this method faced difficulties before. The amplitude of the deformation is well resolved within some fluctuations. Only the initial direction of the oscillation cannot be determined and is matching the true movement by chance. As in the simulations of linear displacements, another parameter is needed here to get the right direction.

Testing the phase-extracting method on oscillatory deformations brings the same results as for the amplitude-extracting method: the amplitude can be well resolved within some fluctuations but the information of the initial direction is lost. Figure 16 illustrates an example of the analysis before choosing the right frequency band. At this point, the data looks quite complex, nevertheless it can be processed further to reconstruct the oscillatory deformation. Besides, the amplitude of the oscillation is quite big here. In contrary to

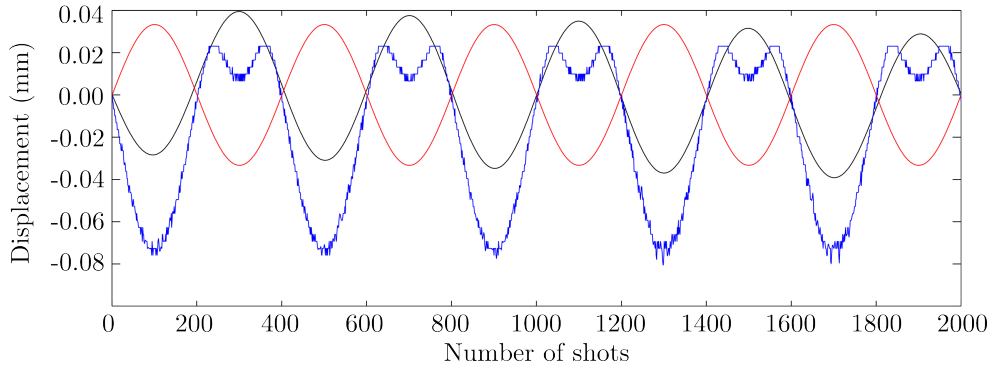


Figure 15: Testing the amplitude-extracting method in a simulated oscillatory deformation experiment. Red: the actual simulated displacement, blue: after matching the amplitudes of the signal to the pulse position, black: the reconstructed displacement.

the linear displacements, where the phase-extracting method had severe problems to resolve big displacements, it here succeeds to reconstruct the original displacement.

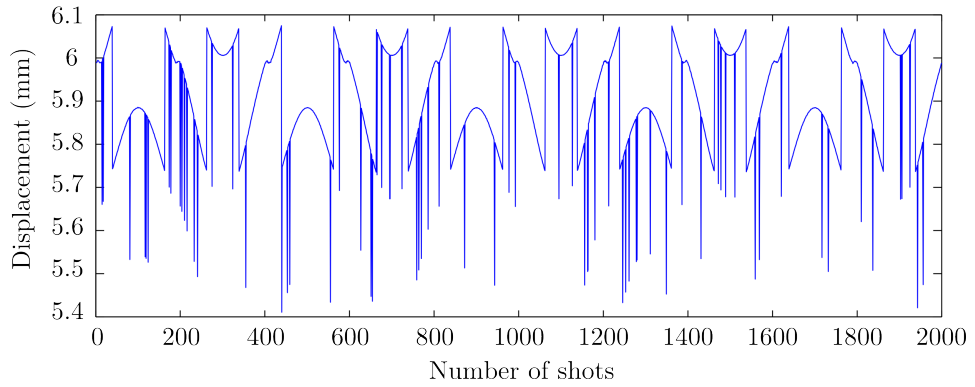


Figure 16: Development of the phase in one speckle point over $n=2000$ signals. This has to be processed further by extracting a low frequency band.

7 Experimental results

The following sections present the experiments, that we carried out and their results. Besides the here listed deformation experiments under different conditions and of different parameters, also static experiments were made to check the processing techniques for possible artifacts. Here, the already in section 6.2 forecast fault of the amplitude-extracting method, when looking for linear deformation and trying to count the oscillations by the absolute phase, to find displacements in signals of just noise was verified. This can be avoided by checking the frequency spectrum before, to verify that a displacement and not only noise is present.

7.1 Linear deformations

First of all, linear deformation experiments are carried out. To do so, the motor is pushing with a constant force, to deform the gel from the edge opposite to the transducer array on. Initially, the array is placed horizontally at middle-height of the gel. The top image in figure 17 shows the deformation field of the gel, calculated by the cross-correlation method, in 3 cm to 6 cm depth from the locked edge, which corresponds in position with the transducer array. One can see directly a quite linear deformation from low displacement on the left side (closer to the locked edge) to higher displacement on right side (closer to the pushing edge).

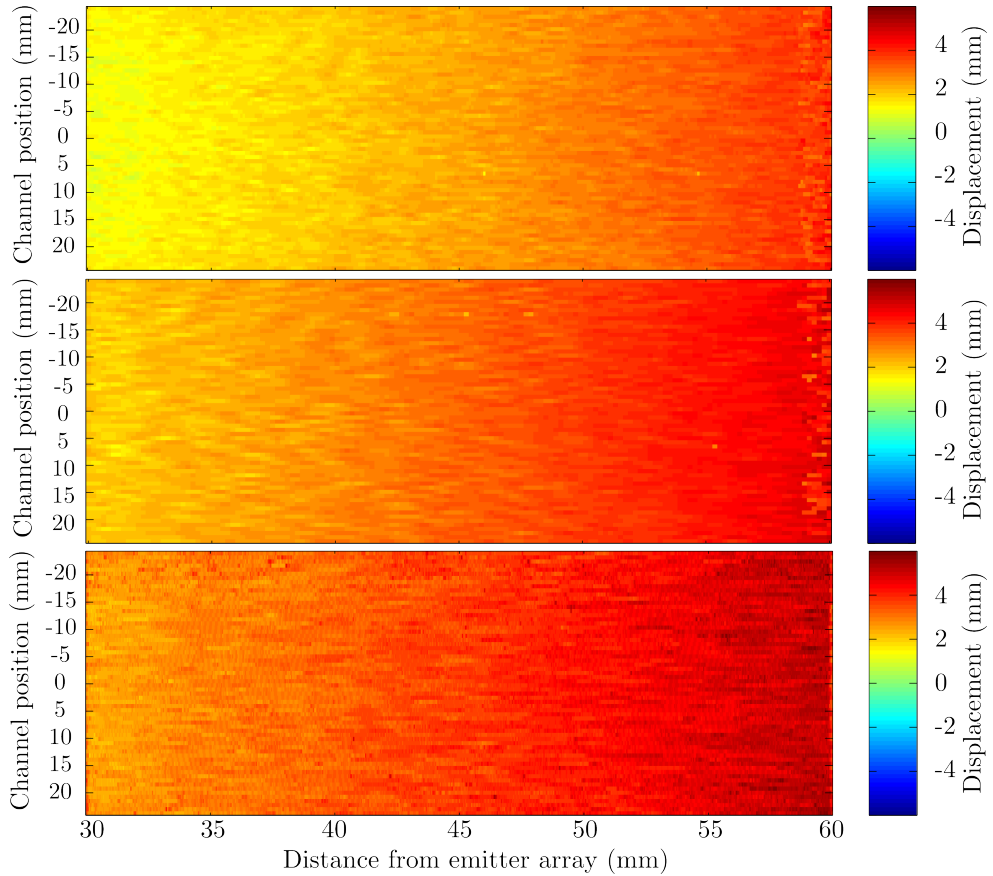


Figure 17: Deformation field inside a gel after linearly compressing it from the side opposite to the transducer array, calculated by different methods: cross-correlation with time window of 50 points (top), cross-correlation with time window of 100 points (middle), amplitude-extracting method (bottom).

To evaluate the different processing techniques and prove their capability, we now compare them with each other and with the displacement of the pushing edge that was measured by the laser. The pushing edge, which is in 8 cm distance from the array, moves by 7.5 cm. Given a linear displacement inside the gel, which can be well assumed in the middle of gel, not close to interfaces where friction forces can occur, the gel should be moved by 2.8 cm at the

30 mm position and by 5.6 cm at the 60 mm position.

The cross-correlation method is carried out twice with time windows of different lengths, namely pulse length and double pulse length. In figure 17 the top image corresponds to the deformation field in the gel calculated by the single pulse length cross-correlation, the image in the middle is calculated by the double pulse length cross-correlation. The results can also be seen in figure 18, where the displacement, averaged over all channels, plotted together with the calculated reference displacement from the laser. Also shown is the analysis of the amplitude-extracting method: the deformation field in the bottom image of figure 17, and the channel mean displacement in figure 18, blue curve. The phase-extracting method is proven to be inconvenient here, as the displacement is too big (compare with section 6.2).

The results of the cross-correlation method show a linear displacement with the right slope compared to the theoretical outcome. However, we have to face a general offset here. Using a time window of single pulse length gives an offset of about 3.0 mm, which is a bit smaller for the double pulse length window with 1.5 mm. The offset is surprising and has so not been foreseeable. A solution for this is not yet found. Just widening the time window can not be the solution as one loses simultaneously spatial resolution. In contrast to this, the amplitude-extracting method does a really good job here. It shows a linear displacement of right slope, which is closest to the calculated one. Furthermore, even though each speckle point is evaluated separately, it gives a really smooth picture.

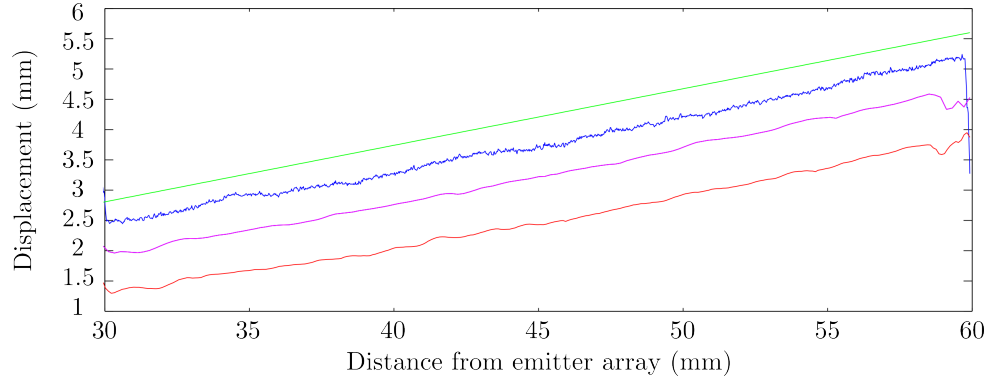


Figure 18: Deformation inside the gel averaged over the array width, calculated by the cross-correlation method (red: time window of pulse length, magenta: time window of double pulse length) and the amplitude-extracting method (blue). Green: Theoretical displacement.

A closer look at the deformation field gained by the cross-correlation shows a slightly bigger displacement on the both sides (recordings of channels towards the ends of the transducer array). This must be justified by a sideways expansion of the gel when squeezed. This is reasonable as the gel is quite incompressible. As a result, it doesn't change in volume when compressed, but rather expands at the free sides. To verify this, a measurement is carried out, in which the transducers array is held on the side to detect displacements

perpendicular to the compression. The clearly confirming result can be seen in figure 19. This means, that scatterers are not only shifted in direction of

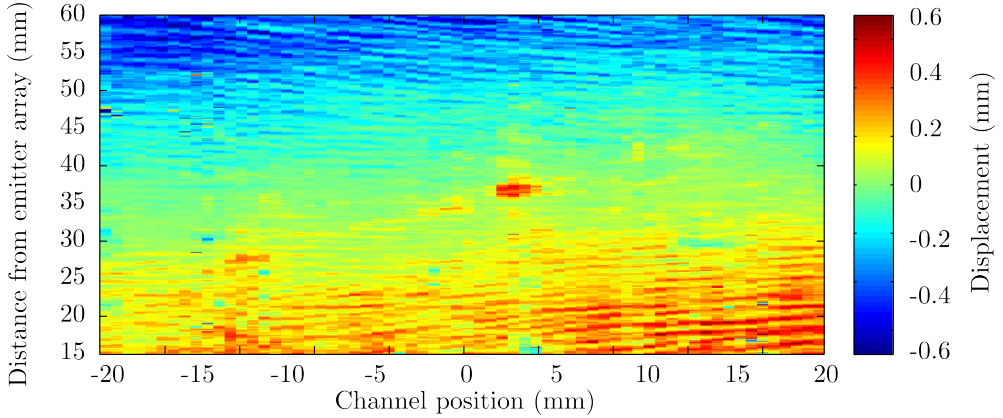


Figure 19: Sidewards displacement inside a gel through compression perpendicular to detected displacement, i.e., here, from the right side.

the compression, but also sideways, especially at positions far from the middle axis. Consequently, the backscattered signals shift not only in transducer direction. This makes successively received signals less coherent, which leads to a rise of the displacement on the sides when using the cross-correlation method. The coherence of the correlation can easily be checked by evaluating the normalised amplitude of the correlation peak. Figure 20 shows the mean correlation coherence of the linear deformation experiment. It shows the expected results of less coherence towards the sides, whereas the overall coherence of above 0.98 is still very high.

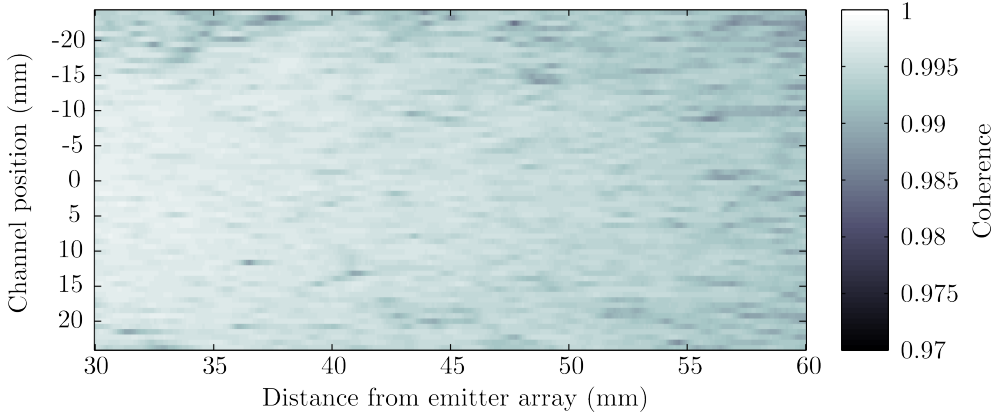


Figure 20: Mean coherence of the cross-correlations for a linear deformation experiment.

7.2 Linear deformations with fixed point

In the following, linear deformation experiments on gels, in which a plastic stick is placed, are presented. The plastic stick is held in place in respect to

the transducer array. The aim of these experiments are both, to test the capability of processing techniques to handle speckle patterns which are influenced by a strong scatterer, and to see the deformation field of the medium around a fixed point. The material of the stick is chosen to be of plastic, as the acoustic impedance of plastic is not as different to the gel as metal would be. In other words, a metal stick would pollute the whole interference pattern more than a plastic stick. The disadvantage of choosing plastic is, that the stick must be of certain thickness in order not to bend under the deformation of the gel. A stick out of metal could have been of much smaller diameter, making it easier to observe the gel behind.

Figure 21 shows the interference pattern of the gel with a plastic stick of 7.5 mm diameter size in the middle, perpendicular to the investigated plane. The stick back-scatters the signal much stronger than the cellulose scatterer. The backscattered signal of the plastic stick is so strong, that it is received and recorded by all the channels. Its actual position is in height between channels 24 and 34. Those channels record first the backscattered signal of the stick, the others with a time delay, which causes the curved shape in the speckle pattern.

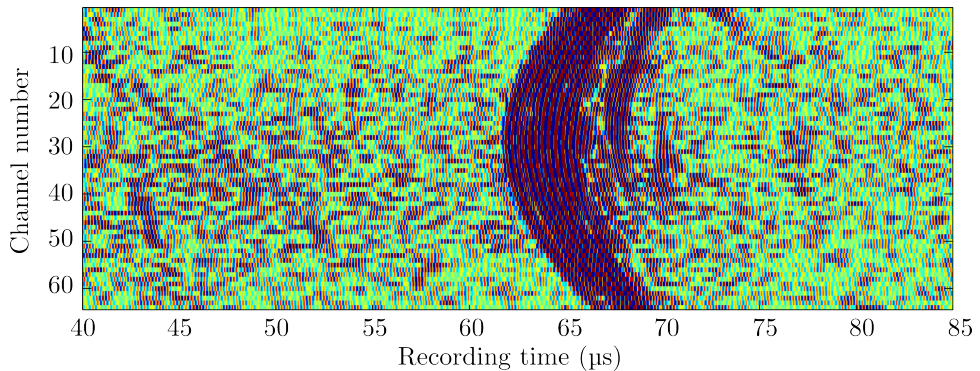


Figure 21: Speckle pattern of a gel with a fixed plastic stick inside.

As the reflection of the plastic stick is much higher in amplitude, movements of scatterers underneath its 'shadow' can no longer be detected. This situation demands a correction of the data to eliminate the pollution. As described in section 5.4, there are two methods which can help out here. Firstly the smoothing of channels method. Figure 22 shows the interference pattern after being smoothed by overlaying each channel by the 5 neighbouring channels from each side. This improves the situation a bit, as the pollution from the strong scatterer is eliminated partly by destructive interference at the curved side wings. Nevertheless, too much pollution remains. Note, that there were electrical faults on the card of the sampling machine, corresponding to the channels 9 to 16. These are visible in the speckle patterns, as well as in the following deformation fields.

To refocus the speckle pattern with such a strong scatterer better, we need to apply the second method. The beam forming method tries to focus all the received signals back to their true origin in the medium. Figure 23 shows the by this reconstructed speckle pattern. It can be seen, that the plastic stick could

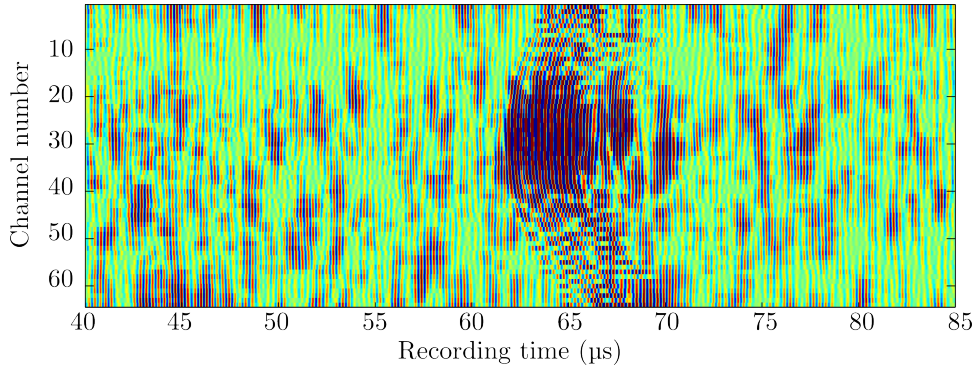


Figure 22: Speckle pattern of a gel with a fixed plastic stick inside, smoothed by adding the five neighbouring channel data of each side to one channel.

be focused on an area of 9.0 mm diameter (converted from the recording time and the channel position). This seems to be a quite good focusing, regarding the stick diameter of 7,5 mm. Still there are some impurities on the sides of the stick and also a slight shadow behind.

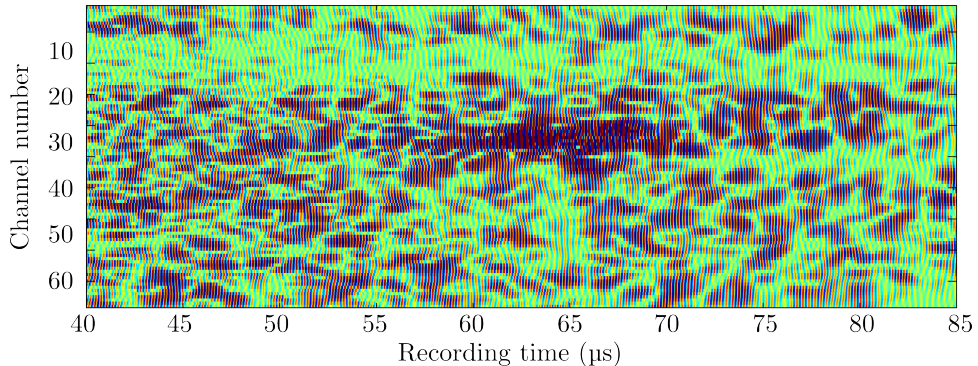


Figure 23: Beamformed speckle pattern of a gel with a fixed plastic stick inside.

The beamformed data can now be further processed as usual. Figure 24 shows the deformation field, here calculated by the correlation method. It's nicely visible, that there is no movement at the position of the stick at around 50 mm from the emitter array and between 0 mm and -5 mm of the channel position. Also in front of the stick towards the transducers there is less displacement than on the sides, which shows, that the deformation of the elastic builds up around the fixed point. However, what is not as expected is the deformation of the gel behind the stick, in point of view from the transducers. There should be a deformation, causing a high stress field, regarding that the gel is exposed to the same deformation over its whole width. At 0 to -5 mm channel position both deformation towards the array and sideways must take place, as compression and shear will occur due to the fixed point. The not detected deformation here must be hidden in the shadow of the plastic stick. The transducer array is not wide enough in order for the beam forming to

focus the signals from behind the stick. In other words it can not look behind the relatively thick stick. Only at the furthest point from the array, small displacements can be detected.

The other processing techniques face problems to evaluate this type of experiment. The phase-extracting method fails due to a too large linear displacement, the cause of failure for the amplitude method is the too small displacement at the position of the stick, where it consequently interprets movement.

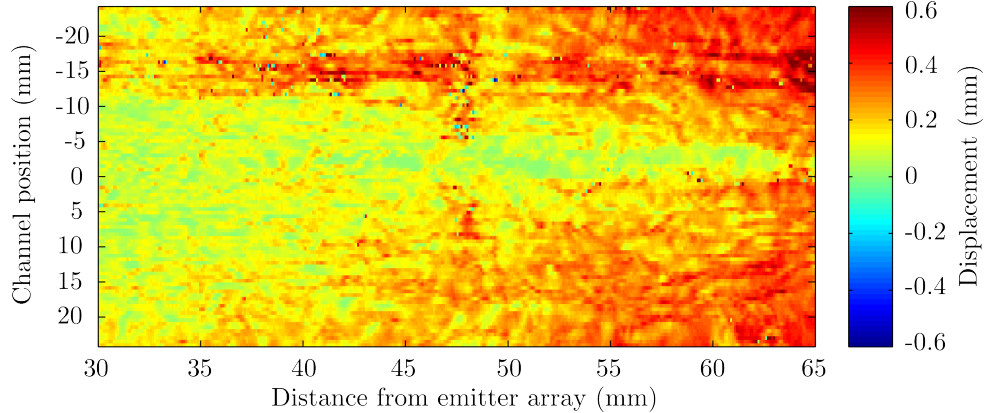


Figure 24: Deformation field inside a gel with a fixed plastic stick inside.

To prove that the zero-displacement at position of the stick is not caused by the strong scattering properties of the plastic stick but truly by its fixed position, another deformation experiment is carried out on a gel with a plastic stick inside. This time, the stick is not fixed, but can freely follow the deformation of the gel. A displacement at the position of the stick proves, that the presence of an strong scatterer, which can be treated by beam forming, doesn't fundamentally falsify the results.

Figures 25 shows the beamformed speckle pattern of the gel with the moveable plastic stick at the begin and at the end of the deformation. One can detect a displacement of the stick towards the transducers of about 5 mm ($\sim 7 \mu\text{s}$). Processing the beamformed data with the correlation method gives the deformation field shown in figure 26. At the position of the stick (at initially 48 mm to 43 mm distance from the transducers) is a displacement clearly visible (even though not of the discussed 5 mm, what is due to the offset in the correlation method). This confirms, that it is not the strong scattering properties of the stick which cause zero-displacement.

What is interesting to see is that one can detect the displacement of the stick itself, but its shadow behind is still visible: a stripe of smaller displacement. The shadow was also observed above in the fixed stick experiment. Now it is shown, that the shadow is not caused by the strong scattering properties, but by the inability of the beam forming method to look behind the stick, at least in the given set-up.

What is left to be noticed is the far smoother picture of the deformation field in the second experiment with the moving stick, compared to the first one

with the fixed stick. This is justified by the far complexer deformation which arises, when a fixed point is present, as more sideways movements inside the gel occur. As a consequence, the signals to correlate are less coherent, what causes a less smooth overall picture.

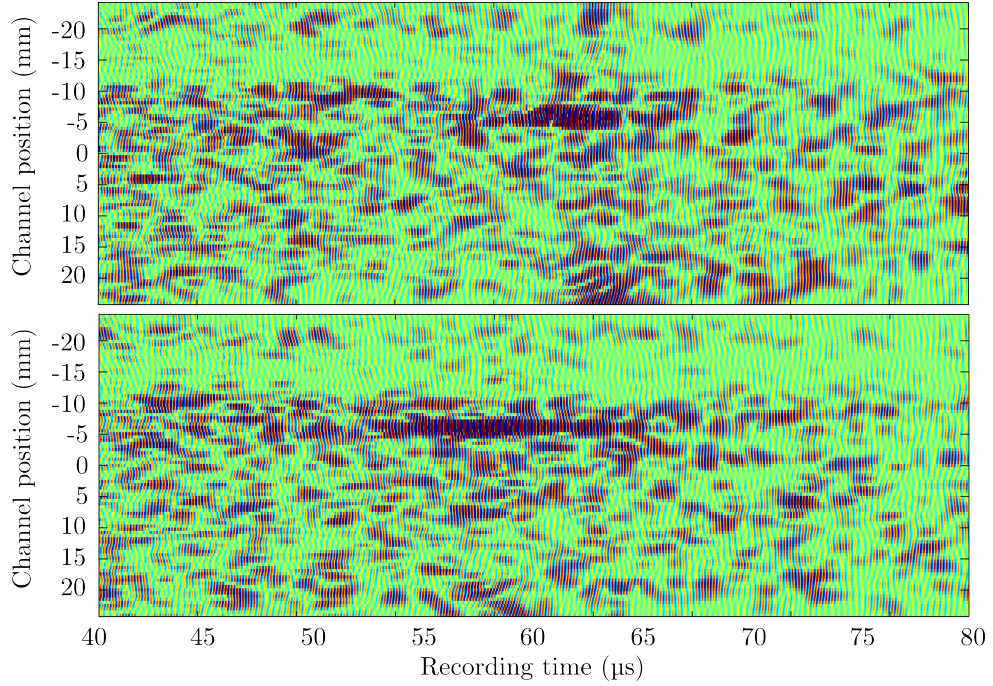


Figure 25: Beamformed speckle pattern of a gel with a not fixed plastic stick inside at the beginning (top) and at the end (bottom) of a deformation.

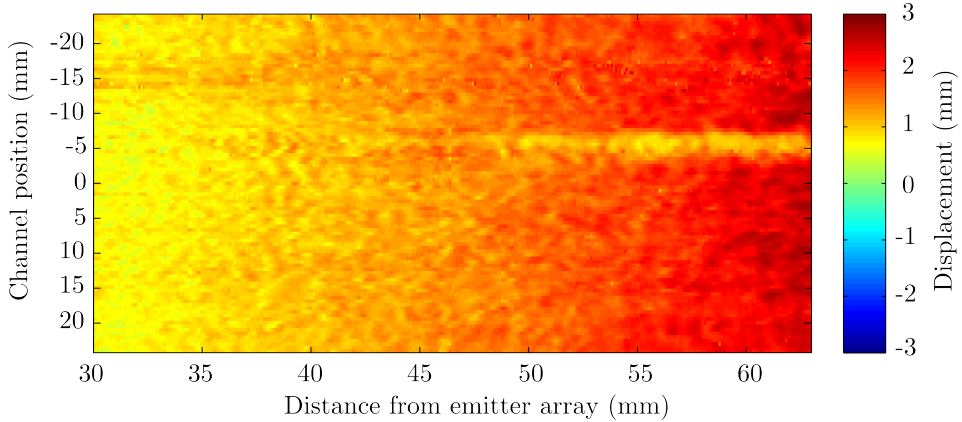


Figure 26: Deformation field inside a gel, carrying a not fixed plastic stick.

7.3 Linear deformations with friction interface

After testing the available processing tools in the two prior sections with specific experiments, we now want to take a look on a more realistic problem. In

order to do this, a stripe of sandpaper is put on half the interface between the gel and the bottom plate. The sandpaper is located next to the locked edge in a fixed position in respect to the transducer array. Like this, the gel faces a highly frictional surface sitting on top of the sandpaper, and a frictionless surface further away from the transducer array, next to the pushing edge. This simulates for example the frictional dynamic in so called subduction zones on earth, where one tectonic plate (e.g. the oceanic crust) moves underneath another tectonic plate (e.g. the continental crust). A high friction zone in the interface between the plates can cause the sticking of an area in the moving plate. If this occurs, high levels of stress are about to build up around the sticking area due to the general push of the moving plate until the friction interface breaks and the stuck area slips. This so caused rupture is one of the main reason of earthquakes. There are several regions on earth, where subduction causes regularly earthquakes, such as on the highly delicate east coast of Japan.

Studies were made to simulate the rupture dynamics, caused by faults of frictional interfaces (e.g. [3],[4]). Here we go one step back and concentrate on the deformation field, caused by a friction area, building up a stress field which can consequently create ruptures.

The experimental set-up includes a stripe of sandpaper on the interface, beginning at the locked edge, ending at a distance of 55 mm. The pushing edge moves linearly towards the locked edge, deforming the gel. Two planes of interests are scanned, parallel above the interface and perpendicular to the interface, detecting movements of the gel in between 35 mm and 70 mm distance from the transducers array (as we are not able to scan the two planes simultaneously, two experiments under the same conditions are carried out). By this, the deformation field of the gel above the boundary from frictionless to frictional interface can be investigated. We expect, that the gel is held by the friction of the sandpaper and doesn't move at this place. Further above the sandpaper, displacement of the gel should increase as the top of the gel is not stuck and should behave as in the previous linear deformation experiments. This means, that the gel is sheared. The shear can be classified as simple shear here, as there is only one direction of the displacement.

Figure 27 shows the result of the measurement, in which the transducer array was positioned vertically, perpendicular to the interface. The image at the top illustrates the deformation field of the scanned plane with the sandpaper located at the bottom (note that there is some pollution from pulse reflections on the rough sandpaper interface at position 40 mm; it could be diminished partly by smoothing the channel data and does not influence the general result). One can recognize clearly the smaller deformation right above the sandpaper. It looks like the deformation builds up around the stuck gel at the frictional interface. The lower image of figure 27 shows the displacement of the gel next to the bottom interface (averaged over 16.5 - 24 mm channel position) and at the top (averaged over -24 - 16.5 mm channel position) along the recorded depth in the gel. As expected, the displacement at the top, where the gel can move freely, develops linearly (red curve), corresponding to a linear deformation, whereas the displacement at the bottom is influenced by the

frictional interface (blue curve). (Note here, that the fitted curves (orange and cyan) are plotted to show the trend of the measurements and do not have a theoretical background.) However, one cannot see a sharp transition from frictionless to frictional interface. The displacement above the sandpaper is not zero, causing a smooth transition between the interfaces. The reason for this is that there is a slight distance between interface and the scanned plane, as the transducer array cannot be positioned closer. Like this, the sharp singularity at the boundary cannot be detected.

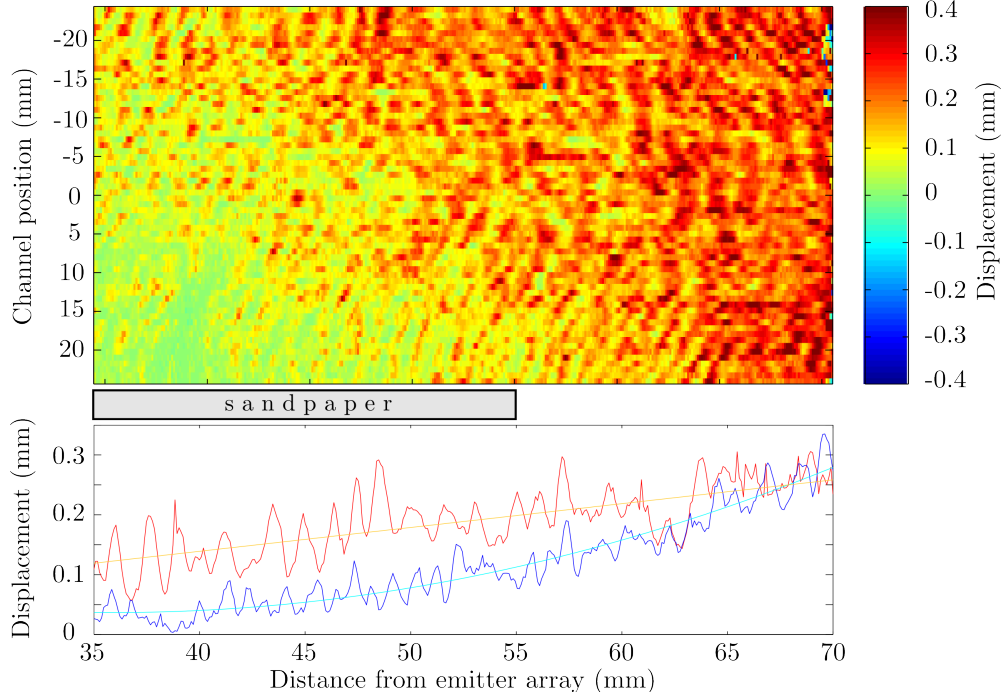


Figure 27: Change of speckle signal over 200 frames, received by one channel.

Figure 28 tries to illustrated the shear in the gel by plotting the displacements against the position above the interface, defined by the channel position. The red curve shows the deformation near the pushing edge, averaged between 63 mm and 70 mm distance from the emitter array. Within general fluctuations the displacement here stays the same at each position above the interface. Above the sandpaper (green curve averaged between 42 mm and 55 mm, blue line from 35 mm to 45 mm) one can clearly see a trend from high displacement at the top of the gel to lower displacement near to the sandpaper. This verifies, that the gel is sheared here. Furthermore it means, that a stress field is build up, as the elastic gel wants back its initial configuration. If the deformation would be increased further, the stress level reaches a point where it is stronger than the (static) friction force of the sandpaper. At this point, the interface would break and the gel would slip, such as the stick-slip events in the subduction zone, causing earthquakes. The deformation inside the gel has also been measured for the horizontal plane, parallel above the interface. By this, one can reconstruct a 3-dimensional illustration of the deformation field inside the gel, how it is shown in figure 29. To reconstruct the deformation

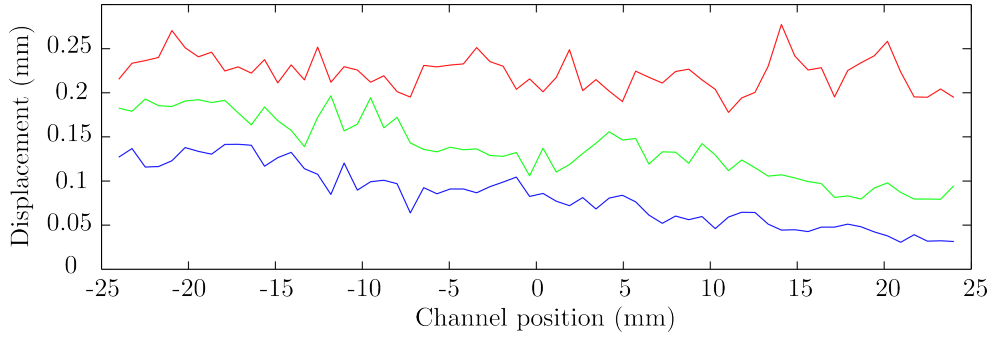


Figure 28: Change of speckle signal over 200 frames, received by one channel.

inside the gel could be a useful tool to simulate stress distribution and thus the cause of rupture events for any kind of configuration (different interfaces, pushing velocities,...).

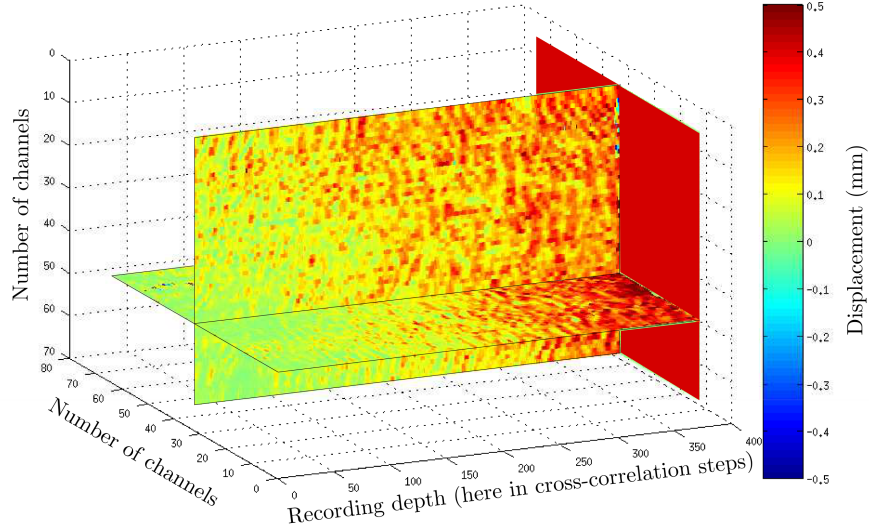


Figure 29: Deformation field inside a gel, which is partly sitting on sandpaper (sandpaper from point 0 to 210 of recording depth). The number of channels (of certain spatial distribution) are defining the width, the number of sampling points (here number of out-carried cross-correlations) the depth in the observed gel.

7.4 Oscillatory deformations

In the previous section, we observed the creation of a deformation field. In this section now, we want to pay attention on the true value of elasticity: returning to the original configuration. Thus, we do not only want to compress the gel, but also release it afterwards. This is carried out by sinusoidal movements of the motor, pushing and releasing the gel bulk from one side. The oscillatory movements of the gel result then in a speckle development as it is shown in

figure 30 of one channel over $n = 2000$ and a certain recording time after each emission. Here one can nicely see four full oscillations, caused by the forth and back movements of the scatterers (in respect to the transducers array).

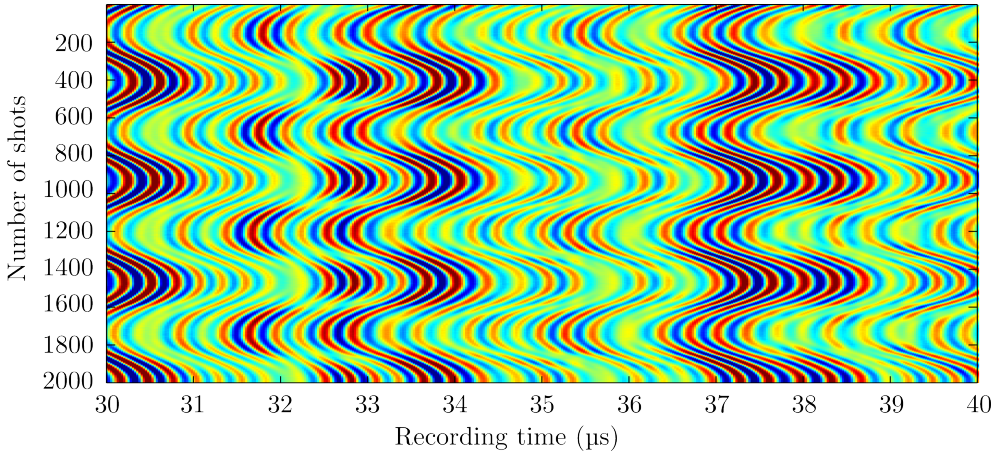


Figure 30: Change of speckle signal over 2000 frames, received by one transducer channel.

The recorded signals are first analysed by the cross-correlation method. The result can be seen in figure 31. The image on the left hand side contains the mean displacement, measured by all the transducer channels, developing over 2000 successive sending-receiving cycles. The image on the right hand side shows separately the displacement of the gel over time (corresponding to the successive shots) near to the pushing edge (red), near to the locked edge (blue), and the displacement of the pushing edge itself, measured by the laser. It is clearly visible, how the elastic gel is compressed and released in full accordance to the movement of the driving edge. As observed in earlier experiments, an increasing displacement of the gel towards the pushing edge is present, whereas the amplitude of the processed signals seems to have again an offset towards lower values, caused by the cross correlation (the locked edge is around 80 mm away from the transducer array, what consequences according to the laser measurements in displacements of 0.4 mm near to the locked edge and 1.1 mm near to the pushing edge). Nevertheless, the oscillatory movement of the gel can nicely be illustrated. Also, the pushing edge is drifting towards the locked edge during the experiments and according to the laser measurement. This drift was unintentional and caused by the inaccurate control of the motor, but it can be resolved by analysing the data, what gives a good feedback for the preciseness in the reconstruction of the gel movement through the cross-correlation.

Secondly, the data is analysed by the amplitude-extracting and phase-extracting method. As described in section 5.2 and 5.3, we select the lowest frequency peak in the spectrum to reconstruct the right oscillation. After this, the initial direction of the oscillation was defined. The results are shown in figure 32. Unfortunately, the amplitude-extracting method doesn't show good re-

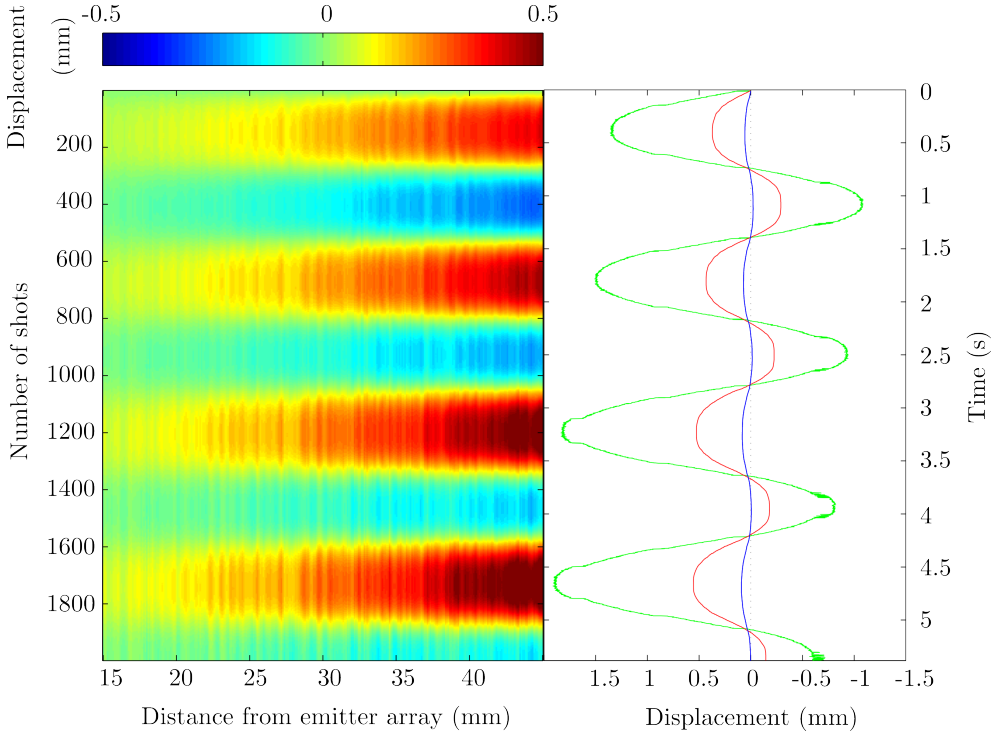


Figure 31: Oscillatory deformation inside the gel, averaged over the width of the transducers array. Left: Displacements over the entire recorded depth in the gel. Right: Displacement near to the oscillating edge (red), near to the locked edge (blue), and of the oscillating edge, measured by a laser (green).

sults at all. The oscillations aren't clearly visible and uncertainties propagate over the successive shots, so that the displacements become even less clear towards the end. Also the amplitude doesn't fit well to the real experimental amplitude. Furthermore, the actual development of low displacement near the locked edge to higher displacements towards the driving edge is not revealed. It seems that the amplitude method faces big problems with irregularities in the experimental data. The simulations before could test the methods how they handle noise, but the underlying pattern was still regular.

The phase-extracting method does a far better job here. The result in the right image of figure 32 shows all the characteristics of the oscillatory deformation, which were also detected by the correlation method: the oscillatory movement of the elastic gel, low displacement near the locked edge, higher displacement towards the driving edge, and also the drift of the driving edge towards the transducer array.

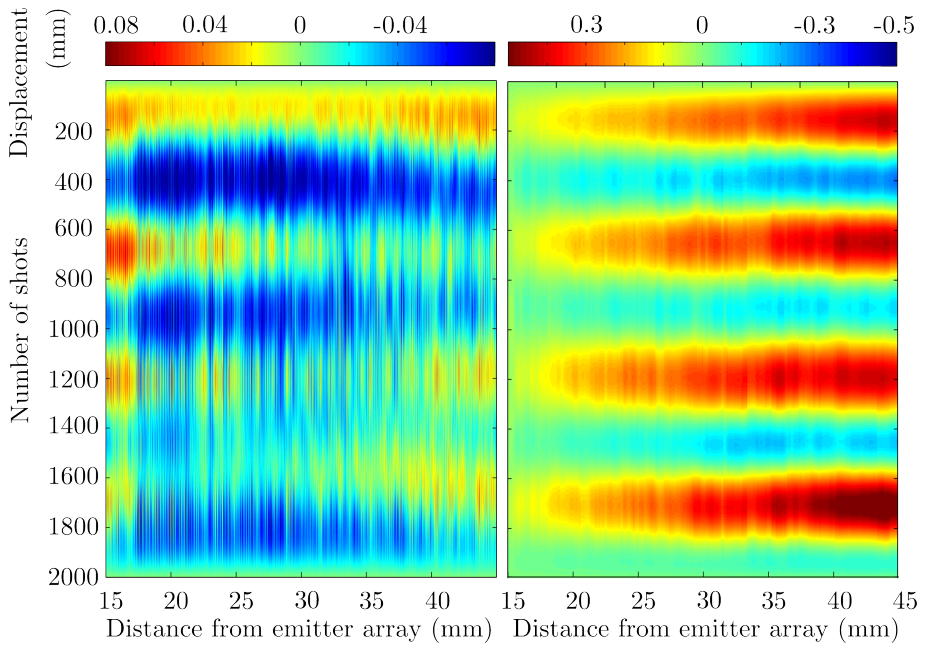


Figure 32: Oscillatory deformation inside a gel, averaged over the width of the transducers array, analysed by the amplitude-extracting method (left) and the phase-extracting method (right).

8 Conclusion

By using pulse-elastography it is possible to visualise deformations inside soft solids. The experiments, which are presented above, contain different kinds of deformation, including deformations of the medium which oscillate over time. All of them could be resolved, whereas the different processing techniques face different problems.

The test of the different methods can be stated as a main outcome of this work, which can be of high interest for further experiments. We conclude, that the cross-correlation method seems to be the most robust one. Using it, one can detect each type of deformation, that is presented in the sections above, even though it has difficulties in calculating the true amplitude of displacement. It probably gains its robustness by making use of both amplitude and phase of recorded signals. The amplitude-extracting and phase-extracting methods seem to work only in certain conditions. They are much more sensible to unpredicted events and do not contain information on the direction of the movement. The high sensibility of the methods might also be of advantage to detect small changes in the signals. Another advantage is that they are much faster than the cross-correlation method which needs a long time to process the data. Because of these two advantages one should remain developing these techniques. Maybe it is possible to combine them and consequently gain robustness.

What also remains to be examined is the elastography in the multiple scattering regime. When the pulse is scattered several times before received by

a transducer, the location of the scatterer gets lost, as the beam doesn't describe a forth and back path. On the other hand one can gain sensibility, as the signal changes in a higher magnitude than in the single scattering regime, when one scatterer is moved. If one would succeed to process signals after multiple scattering, this would bring further possibilities to the elastography method, as one could study much more materials.

Also the investigation of deformation fields should be continued, to also evaluate the deformation under more complex conditions. This will be of high interest for seismology in order to get a better understanding of the heterogeneous stress fields, that cause ruptures.

References

- [1] SARVAZYAN, A. P. et al., Ultrasound in Medicine & Biology **24** (1998) 1419 .
- [2] SANDRIN, L. et al., Ultrasonic imaging **21** (1999) 259.
- [3] CAMPILLO, S. et al., EPL (Europhysics Letters) **96** (2011) 59003.
- [4] LATOUR, S. et al., Journal of Geophysical Research: Solid Earth **118** (2013) 5888.
- [5] GALLOT, T., Imagerie acoustique en milieux réverbérants, 2010.
- [6] HASSAN, C. et al., Structure and applications of poly(vinyl alcohol) hydrogels produced by conventional crosslinking or by freezing/thawing methods, in *Biopolymers & PVA Hydrogels, Anionic Polymerisation Nanocomposites*, volume 153 of *Advances in Polymer Science*, pages 37–65, Springer Berlin Heidelberg, 2000.
- [7] KATO, K. et al., Liver International **28** (2008) 1264.
- [8] NORDLING, C. et al., Lund (2006).
- [9] RIVET, D. et al., Geophysical Research Letters **38** (2011) .

List of Figures

1	Illustration of the definition of Young's modulus (left) and shear modulus (right) (extracted from [7]).	5
2	Bulk- and shear moduli of different tissues, dependent on the applied pressure (extracted from [1]).	6
3	Real-time tissue elastography (left) is used to detect a tumour inside the liver, which cannot be resolved by ultrasonography (right). The tumour is visible in blue colour, as it is harder than the surrounding liver tissue (extracted from [7]).	6
4	Illustration of the imaging technique: a transducer array is emitting a pulse into the scattering medium. Backscattered signals arrive at different times by the same array. The signals are sampled at 40 MHz. The image in the middle shows the so recorded signal in one channel. The bottom image contains the same informations of a zoomed time section. This record will form with the records of the other channels the so called speckle pattern.	8
5	Illustration of the speckle pattern created by backscattered pulses, received by 64 channels over a defined recording time. This pattern is created after each of n successive sent signals.	9
6	Change of a speckle signal over 40 frames, received by one channel.	10
7	Proof of the single scattering regime in the gel by visualization of the strong reflection from a metallic plate behind (from 102 μ s on).	11
8	Backscattered signals of two successive pulse shots in a scattering medium, which is displaced in between the shots, causing a delay of the signals in the recording time.	12
9	On top the oscillations of one speckle point during a linear deformation experiment of $n = 1000$ signal emitting-receiving cycles. Bottom image shows the corresponding wrapped phase (red) and absolute phase (blue).	13
10	Smoothing of channels by overlaying them, as they receive the backscattered signal of the same scatterer.	15
11	Backscattered signal of a strong scatterer is received in many channels and thus causes the requirement of beam forming.	16
12	According to the delay in arriving of a signal between the channels, the data is shifted. Before overlaying them, the signal amplitude is weighed, putting more emphasis on the channel that receives the directional backscattered signal.	16
13	Sketch of the experimental set-up.	17
14	Testing the phase-extracting method in a simulated linear deformation experiment. Red: the actual simulated displacement, black: the result of the analysis by the phase-extracting method.	18

15	Testing the amplitude-extracting method in a simulated oscillatory deformation experiment. Red: the actual simulated displacement, blue: after matching the amplitudes of the signal to the pulse position, black: the reconstructed displacement.	19
16	Development of the phase in one speckle point over $n=2000$ signals. This has to be processed further by extracting a low frequency band.	19
17	Deformation field inside a gel after linearly compressing it from the side opposite to the transducer array, calculated by different methods: cross-correlation with time window of 50 points (top), cross-correlation with time window of 100 points (middle), amplitude-extracting method (bottom).	20
18	Deformation inside the gel averaged over the array width, calculated by the cross-correlation method (red: time window of pulse length, magenta: time window of double pulse length) and the amplitude-extracting method (blue). Green: Theoretical displacement.	21
19	Sidewards displacement inside a gel through compression perpendicular to detected displacement, i.e., here, from the right side.	22
20	Mean coherence of the cross-correlations for a linear deformation experiment.	22
21	Speckle pattern of a gel with a fixed plastic stick inside.	23
22	Speckle pattern of a gel with a fixed plastic stick inside, smoothed by adding the five neighbouring channel data of each side to one channel.	24
23	Beamformed speckle pattern of a gel with a fixed plastic stick inside.	24
24	Deformation field inside a gel with a fixed plastic stick inside.	25
25	Beamformed speckle pattern of a gel with a not fixed plastic stick inside at the beginning (top) and at the end (bottom) of a deformation.	26
26	Deformation field inside a gel, carrying a not fixed plastic stick.	26
27	Change of speckle signal over 200 frames, received by one channel.	28
28	Change of speckle signal over 200 frames, received by one channel.	29
29	Deformation field inside a gel, which is partly sitting on sandpaper (sandpaper from point 0 to 210 of recording depth). The number of channels (of certain spatial distribution) are defining the width, the number of sampling points (here number of out-carried cross-correlations) the depth in the observed gel.	29
30	Change of speckle signal over 2000 frames, received by one transducer channel.	30
31	Oscillatory deformation inside the gel, averaged over the width of the transducers array. Left: Displacements over the entire recorded depth in the gel. Right: Displacement near to the oscillating edge (red), near to the locked edge (blue), and of the oscillating edge, measured by a laser (green).	31

- 32 Oscillatory deformation inside a gel, averaged over the width
of the transducers array, analysed by the amplitude-extracting
method (left) and the phase-extracting method (right). 32